



RESEARCH PAPER

Effect of epistasis and environment on flowering time in barley reveals a novel flowering-delaying QTL allele

Nazanin P. Afsharyan¹, Wiebke Sannemann², Jens Léon¹, and Agim Ballvora^{1,*}

¹ Institute for Crop Science and Resource Conservation, Chair of Plant Breeding, University of Bonn, 53115 Bonn, Germany

² Chair of Plant Breeding, Martin Luther University Halle-Wittenberg, 06120 Halle, Germany

* Correspondence: ballvora@uni-bonn.de

Received 2 June 2019; Editorial decision 11 October 2019; Accepted 7 October 2019

Editor: Fabrizio Costa, Fondazione Edmund Mach, Italy

Abstract

Flowering time is a complex trait and has a key role in crop yield and adaptation to environmental stressors such as heat and drought. This study aimed to better understand the interconnected dynamics of epistasis and environment and look for novel regulators. We investigated 534 spring barley MAGIC DH lines for flowering time at various environments. Analysis of quantitative trait loci (QTLs), epistatic interactions, QTL × environment (Q×E) interactions, and epistasis × environment (E×E) interactions were performed with single SNP and haplotype approaches. In total, 18 QTLs and 2420 epistatic interactions were detected, including intervals harboring major genes such as *Ppd-H1*, *Vrn-H1*, *Vrn-H3*, and *denso/sdw1*. Epistatic interactions found in field and semi-controlled conditions were distinctive. Q×E and E×E interactions revealed that temperature influenced flowering time by triggering different interactions between known and newly detected regulators. A novel flowering-delaying QTL allele was identified on chromosome 1H (named ‘HvHeading’) and was shown to be engaged in epistatic and environment interactions. Results suggest that investigating epistasis, environment, and their interactions, rather than only single QTLs, is an effective approach for detecting novel regulators. We assume that barley can adapt flowering time to the environment via alternative routes within the pathway.

Keywords: Barley, environmental effect, epistasis, flowering time, MAGIC population, novel QTL, QTL analysis.

Introduction

Flowering time indicates the transition from the vegetative to the reproductive phase in plants (Mouradov *et al.*, 2002), and as a major determinant for biomass accumulation and grain filling period length, affects grain yield. It was targeted during crop domestication and breeding to adapt wild ancestors of modern cultivars (Ross-Ibarra *et al.*, 2007). Barley (*Hordeum vulgare* ssp. *vulgare* L.) is the fourth most cultivated cereal worldwide and is consumed for food, feed, and the malting process (Schulte *et al.*, 2009). The flowering time regulatory network of barley, as a model for small-grain cereals, is relatively well described (International Barley Genome Sequencing Consortium, 2012). However, there is currently

relatively little available information about the genes involved in this network, and their epistatic and environmental interactions, compared with the dicot model plant *Arabidopsis thaliana* (Blümel *et al.*, 2015). Flowering time regulators belong to a complex network of genes that interact with environmental cues (Putterill *et al.*, 2004). Focusing on the whole system of interacting factors, which includes genes and environment, could offer more informative solutions that provide new insights to identify novel regulators (Blümel *et al.*, 2015; Valentim *et al.*, 2015).

The multiparent advanced generation inter-cross (MAGIC) strategy was designed to improve power and precision in

quantitative trait locus (QTL) mapping and overcome limitations of populations derived from biparental crossing systems by providing extensive genetic variance (Cavanagh *et al.*, 2008). MAGIC populations are constructed by linkage-based design and multiple generations of recombinations, which provide high genetic mapping power and resolution (King *et al.*, 2012). Common statistical methods for QTL and epistatic interactions using molecular markers such as single nucleotide polymorphisms (SNPs) have been used successfully with MAGIC populations in *A. thaliana* (Kover *et al.*, 2009), wheat (Huang *et al.*, 2012), rice (Bandillo *et al.*, 2013), and winter wheat (Mackay *et al.*, 2014). However, the involvement of more than two parents and their possible genetic similarities pose statistical challenges for analyzing the effects of parental alleles (Sannemann *et al.*, 2015). SNP data from progenies can be transformed to a recognizable parental pattern of content, also known as the ‘haplotype phase’, for mapping purposes (Browning and Browning, 2011). Recent efforts have been made to use both single SNP and haplotype-phase analysis to provide sufficient mapping power (Sannemann *et al.*, 2015; N’Diaye *et al.*, 2017; Ogawa *et al.*, 2018). A spring barley MAGIC population was constructed using an eight-way cross of seven barley landraces and one elite cultivar. This population was used to study flowering time QTL (Sannemann *et al.*, 2015) and epistatic interactions (Mathew *et al.*, 2018) in pot experiments, which detected regions harboring major flowering time genes such as *Vrn-H1* and *Vrn-H3*.

Flowering time in barley is regulated by photoperiod and vernalization as well as environment-independent pathways such as earliness *per se* (EPS) (Cockram *et al.*, 2007). Under long-day conditions, one of the key regulators that responds to photoperiod is *PSEUDO-RESPONSE REGULATOR* (*HvPRR37*), also known as *PHOTOPERIOD RESPONSE LOCUS1* (*Ppd-H1*). It functions in the circadian clock oscillator and is orthologous to clock gene *PRR7* in *Arabidopsis* and *osPRR37* in rice (Turner *et al.*, 2005). *Ppd-H1* interacts with *CONSTANS* (CO) and promotes flowering by initiating expression of *Vrn-H3*, a homolog of *A. thaliana* *FLOWERING LOCUST* (*FT*) (Yan *et al.*, 2006). *Vrn-H3* functions at the intersection of three main pathways—vernalization, photoperiod, and circadian clock (Campoli *et al.*, 2012)—and is involved in the development of the reproductive apex and inflorescence (Faure *et al.*, 2007; Digel *et al.*, 2015). Another major gene upstream of *Vrn-H3*, encoding an *APETALA1* family MADS-box transcription factor, *Vrn-H1*, is a positive regulator of flowering time in response to temperature (Distelfeld *et al.*, 2009) that induces flowering time by promoting the transition from the vegetative to the reproductive phase (Hemming *et al.*, 2008). Epistasis between *Vrn-H1* and *Vrn-H3*, and the effect of lower temperature on promoting *Vrn-H1*, is an example of flowering time control beyond the effect of single genes (Hemming *et al.*, 2008; Cockram *et al.*, 2015). Epistasis is the term used to describe different levels of interactions among genes, including the functional interaction (protein level), allelic variation affecting the pathway (gene level), and deviations from additivity detected by statistical models (Phillips, 2008). Most mapping studies have successfully introduced novel regulators by focusing on single QTL (Bezant *et al.*, 1996; Pillen

et al., 2003; Wang *et al.*, 2010; Alqudah *et al.*, 2014; Sannemann *et al.*, 2015; Maurer *et al.*, 2016). Few reports have described epistatic interactions in the flowering time pathway of barley (Maurer *et al.*, 2015; Mathew *et al.*, 2018). Thus, the effects of epistasis and environment and their collective contribution to flowering time are not well understood. To provide more detailed insights into the flowering time regulation network in barley, using strategies beyond single QTL analysis is crucial.

The main aim of this study was to investigate the effect of epistasis and environment on flowering time in barley to detect novel mediators. Objectives of the study were (i) to investigate epistatic interactions under different environments in field and semi-controlled conditions, (ii) to investigate the effect of environment on the timing of flowering, by analyzing QTL \times environment and epistasis \times environment interactions, and (3) to shed light on novel flowering time regulator(s) involved in epistatic and/or environment interactions.

Materials and methods

Plant material

The MAGIC population was constructed by inter-crossing eight barley (*Hordeum vulgare* ssp. *vulgare*) genotypes, including one plant from each of seven landraces, Ackermanns Bavaria IPK No. HOR 100 (Ack. Bavaria), Ackermanns Danubia IPK No. BCC 1427 (Ack. Danubia), Crieewener 403 IPK No. HOR 62, Heils Franken IPK No. BCC 1433, Heines Hanna IPK No. HOR 59, Pflugs Intensiv IPK No. BCC 1441, and Ragusa IPK No. BCC 1359, and the elite cultivar Barke, in an eight-way cross. Then, double haploid (DH) lines were produced as described in Sannemann *et al.* (2015). Ragusa represents a facultative and the others are spring barley ecotypes. The landraces used in this cross have contributed as founders of German barley cultivars.

Experimental setup and phenotypic data

Data for days to heading were collected under field and semi-controlled conditions. Field trials were conducted in 2016 and 2017 at Campus Klein-Altendorf (50°36′46.6″N, 6°59′39.7″E) of the University of Bonn. The lines were sown on 11 April 2016 (mean temperature 12.14 °C), and 3 April 2017 (mean temperature 8.63 °C). An unreplicated experimental design with a check every third plot (Mangelsdorf, 1953; Warner, 1953; Federer, 1956a) was employed, which is the standard design used for early-generation field trials in breeding programs (Federer, 1956b, 1993). The DH lines were completely randomized. The eight parents and cultivar scarlet were also randomized as controls. Each DH line was sown in one row containing 10 plants. Each plot was 1 m \times 1.5 m in size and contained six DH lines, and the space between plots was 1 m. Field trials were subjected to fertilization and pest management following local practices. All DH lines reached the heading stage and the flowered plants for each line were counted; 99% had at least four plants that headed and were considered for data collection. The number of heading plants per DH line was on average six or seven for both years. The setup for semi-controlled conditions for the experiments conducted in 2011 and 2012, which were done under a foil tunnel at Campus Poppelsdorf (50°43′34.1″N, 7°05′14.6″E) of the University of Bonn, is detailed in Sannemann *et al.* (2015). The sowing dates were 4 April 2011 (mean temperature 11.99 °C), and 3 April 2012 (mean temperature 12.51 °C). Days to heading (BBCH 49; Hack *et al.*, 1992) was scored as the number of days after sowing when at least 50% of plants of each DH line showed 3 cm of awns. The data for each year were analyzed separately. Phenotypic data are provided in Dataset 1 available at Dryad Digital Repository (<https://doi.org/10.5061/dryad.g25cm28>; Afsharyan *et al.*, 2020). To evaluate the effect of environment, the daily average temperature for 100 days after sowing was measured for the 4 sowing years (2011, 2012, 2016, and

2017) to calculate growing degree-days (GDD), using base temperature 3 °C (Schelling *et al.*, 2003), for each growing season (Dataset 2 at Dryad).

DNA extraction and genotyping

DNA was isolated from each barley MAGIC DH line according to the protocol for Diversity Arrays Technology marker analysis (<https://www.diversityarrays.com>) and prepared as described by Sannemann *et al.* (2015). Then, DNA samples were genotyped using the 9k iSelect SNP array (Comadran *et al.* 2012) at TraitGenetics GmbH (Stadt Seeland OT, Gatersleben, Germany) (Dataset 3 at Dryad). The processing of raw genotypic data was done as described by Sannemann *et al.* (2015). Genotypes with less than 10% missing values were included and missing data were imputed according to the mean imputation approach (Rutkoski *et al.*, 2013). Then, the genotyping dataset was constructed by eliminating markers with a minor allele frequency (MAF) of less than 1%. Finally, 5199 SNP markers were used for further analysis. Due to the inclusion of more SNPs in this study than in the study of Sannemann *et al.* (2015), the SNPs were haplotyped in two groups and then collected in one dataset. Construction of haplotype data using SNPs with MAF $\geq 5\%$ was performed as described by Sannemann *et al.* (2015). The remaining SNPs ($5\% > \text{MAF} \geq 1\%$) were haplotyped by the K-means clustering method using Proc Fastclus in SAS 9.4 (SAS Institute Inc., Cary, NC, USA). The SAS script and sample data are provided in Method 1 at Dryad. Then, manual corrections were made by comparing the phase patterns of parents and DH lines to improve data accuracy and resolution of the haplotype data. Finally, 4557 SNP markers with missing haplotype-phase data $\leq 15.5\%$ were used for further analysis. *In silico* analysis was performed using the IPK barley BLAST server (https://webblast.ipk-gatersleben.de/barley_ibsc/) (Colmsee *et al.*, 2015).

Statistical analysis

Analysis of phenotypic data

Descriptive statistics was performed in R software (R Core Team, 2015) by using the following core generic functions in R: summary to calculate minimum, maximum, and mean; std.error, sd, and var to calculate standard error, standard deviation (SD), and coefficient of variation (CV), respectively. Analysis of row and column effect was conducted in R with the lm function from the package stats by considering non-replicated MAGIC DH lines, row, column, and controls as fixed effects. The same R function was used to perform analysis of variance (ANOVA) for days to heading by taking DH lines and year as fixed effect. The GDD accumulation in the 100 days after sowing was compared among years by a paired Student's *t*-test. In addition, the relationship between days to heading and the respective GDD (flowering time GDD) of genotypes was tested by using Pearson's correlation coefficient (*r*). Variance components were estimated using the PROC VARCOMP procedure (all effects as random) in SAS 9.4. Heritability (h^2) was calculated as:

$$h^2 = \frac{V_G}{V_G + \frac{V_{GY}}{y} + \frac{V_E}{y}}$$

where V_G : variance of genotype, V_{GY} : variance of genotype \times year, V_E : variance of experimental error, and y : number of years.

QTL mapping and QTL \times environment interaction models

QTL analysis and QTL \times environment interaction through single SNP analysis (single SNP approach; SA) and haplotype analysis (haplotype approach; HA) was conducted, using the PROC MIXED procedure in SAS 9.4, by the following linear model:

$$Y_{ij} = \mu + M_i + C_j + M_i \times C_j + \varepsilon_{ij}$$

where Y_{ij} : response variable; μ : general mean; M_i : the fixed effect of the *i*th marker genotype; C_j : the fixed effect of the *j*th calendar year; $M_i \times C_j$: the fixed interaction effect of the *i*th marker genotype with the *j*th calendar year; and ε_{ij} : the residual. To reduce the number of detected false positives, the multilocus procedure, as an efficient selection strategy, was

implemented within the model (Sillanpää and Corander, 2002; Kilpikari and Sillanpää, 2003; Bauer *et al.*, 2009). This process is composed of a forward selection procedure that inserts the most informative SNP inside the model in each iterative cycle, then uses it to re-analyze the remaining SNPs. The results of each round are considered as the basis for the next round of the forward selection process, and iteration of the multilocus QTL model continues until no other SNP is detected. Additionally, the control of QTL false discovery rate (FDR) was incorporated inside the model, which was conducted by using the PROC MULTTEST procedure in SAS 9.4. A threshold of *P*-value ≤ 0.001 with 1000 permutations and FDR value ≤ 0.05 was determined (Doerge and Churchill, 1996). Due to strong decay in linkage disequilibrium, a confidence interval of 3.5 cM and 15 cM was defined on both sides of the most significant SNP marker in SA and HA, respectively. The model defined QTL intervals by clustering SNPs based on their significance in the first iteration of the multilocus procedure. To test the significance of QTLs, a 'leave20%out' cross-validation procedure that randomly left out 20% of the genotypes from the original dataset and re-analyzed the remaining genotypes was performed. This process was executed 20 times and a new *P*-value was calculated using the mean of all. For analysis of QTL \times environment interactions across 4 years, five times cross-validation was used. The SAS script employed for QTL and QTL \times environment interaction analysis, including implementation of FDR and cross-validation procedures, is provided in Method 2 at Dryad. Genetic variance explained by a single SNP marker (R_M^2) was calculated as:

$$R_M^2 = \text{SQ}_M / \text{SQ}_g$$

where SQ_M is the sum of squares of M_i and SQ_g was calculated as the type I sum of squares of the DH lines in an ANOVA model (von Korff *et al.* 2006). Finally, the total proportion of explained genetic variance was estimated.

Epistatic interaction and epistasis \times environment interaction models

A two-way epistatic interaction multilocus approach and epistasis \times environment interaction was performed through SA and HA in SAS 9.4. A threshold of *P*-value ≤ 0.001 and FDR value ≤ 0.05 was set followed by cross-validation using a hierarchical model:

$$Y_{ijk} = \mu + M1_i + M2_j + M1_i \times M2_j + C_k + M1_i \times M2_j \times C_k + \varepsilon_{ijk}$$

where Y_{ijk} : response variable; μ : general mean; $M1_i$ and $M2_j$: fixed effects of the *i*th marker genotype and the *j*th marker genotype, respectively; $M1_i \times M2_j$: the fixed interaction effect of the *i*th $M1$ marker genotype with the *j*th $M2$ marker genotype; C_k : the fixed effect of the *k*th calendar year; $M1_i \times M2_j \times C_k$: the fixed interaction of the *i*th $M1$ marker genotype with the *j*th $M2$ marker genotype and the *k*th calendar year; and ε_{ijk} : the residual. The SAS script for epistatic interaction and epistasis \times environment interaction analysis, including implementation of FDR and cross-validation procedures, is provided in Method 2 at Dryad. Genetic variance explained by a single interaction was analyzed by fitting the model same as genetic variance by a single QTL. Subsequently, the total proportion of genetic variance explained by interactions was calculated.

Results

Flowering time under various environmental conditions

To study flowering time and the effect of environment on it, days to heading was scored in the spring barley MAGIC DH lines grown under field and semi-controlled conditions. Flowering time in the field showed a large phenotypic variation of more than 30 days each year, which was more diverse

than that of the parents. Under semi-controlled conditions, the range of flowering time was shorter than under field conditions for both the DH lines and the parents, resulting in a higher CV (%) under field conditions (Table 1). Row and column effects were not significant in all experiments. ANOVA for years revealed highly significant differences ($P < 0.01$) (see Table 1 at Dryad). Evaluation of GDD accumulation for 100 days after sowing by a paired Student's *t*-test showed a significant difference between years. GDD accumulated faster in the foil tunnel conditions during the growing seasons, corresponding to an earlier flowering time (Fig. 1A; Table 2 at Dryad). Daily average temperature for the first 2 weeks after sowing was measured in the 4 sowing years to investigate the effect of lack of vernalization (which requires temperatures in the range 4–12 °C), which can delay flowering in some genotypes (Trione and Metzger, 1970). Flowering time was not accelerated in the years in which there was a lower number of days with mean temperature higher than 12 °C. Furthermore, Pearson's correlation coefficient between days to heading and GDD was >0.99 for each year. The DH lines were subjected to the same day length each year as a result of very similar sowing dates (Fig. 1B).

Identification of QTL for flowering time under field conditions

To identify genetic regions that control flowering time, the association between phenotypic and genotypic data was evaluated. The results revealed 11 QTLs by SA (Fig. 2A) and 7 QTLs by HA (Fig. 2B). All seven chromosomal regions found by HA were also detected by SA. One QTL on chromosome 2H was associated with earlier flowering by 8.79 days (Tables 2 and 3). QTLs detected with SA and HA explained in total 48.43% and 52.92% of the genetic variance, respectively. One single parent was the source of five loci mapped by both SA and HA on chromosomes 1H, 2H, 3H, 5H, and 7H (Tables 2 and 3). According to SA, the strongest association with flowering time was detected on chromosome 7H at 34.35 cM (BOPA2-12-30895), and explained 9.96% of the genetic variance (Table 2). For HA, the most significant QTL was mapped to chromosome 2H at 27.69 cM (SCRI_RS_140819), and explained

14.96% of the genetic variance (Table 3). The alleles for both loci originated from the parental line Ragusa.

Identification of epistatic interactions under field and semi-controlled conditions

To evaluate how the interaction among genetic loci affects flowering time, genome-wide epistatic interaction analysis was performed. In total, 55 and 27 epistatic interactions were detected ($P \leq 0.1E-15$) under field conditions by SA (Fig. 3A; Table 3 at Dryad) and HA (Fig. 3B; Table 4 at Dryad), respectively. The most significant epistatic interaction was between two regions located on chromosomes 7H (34.35 cM, SA; 37.61 cM, HA) and 2H (18.91 cM, SA; 27.69 cM, HA). This interaction affected flowering time by more than 20 days and explained 28.13% and 38.02% of the genetic variation by SA and HA, respectively. Both of the alleles causing the polymorphism originated from the parental line Ragusa; the one on chromosome 2H induced earlier flowering, whereas the one on chromosome 7H delayed flowering time (see Table 4 at Dryad).

Analysis of epistatic interactions under foil tunnel conditions revealed 1139 and 1199 interactions ($P \leq 0.1E-15$) using SA (Fig. 3C; Table 5 at Dryad) and HA (Fig. 3D; Table 6 at Dryad), respectively. Both analyses identified the same interacting regions on chromosomes 7H (32.79 cM, SA; 32.79 cM, HA) and 5H (125.49 cM, SA; 118.75 cM, HA) as the most significant ones. This interaction influenced flowering time by more than 4 days in both approaches, and explained 26.94% and 42.01% of the genetic variance by SA and HA, respectively (Tables 5 and 6 at Dryad). The allele on chromosome 5H contributed to earlier flowering whereas the one on chromosome 7H delayed flowering time (Table 6 at Dryad); both originated from the parental line Ragusa.

Detection of HvHeading, a novel flowering-delaying QTL allele

To distinguish the novel QTL, the detected loci in this study were compared with previously reported regions. SA and HA consistently revealed a novel QTL

Table 1. Descriptive statistics and heritability for days to heading (DHE) for the parental lines and the spring barley MAGIC DH lines under foil tunnel (2011 and 2012) and field (2016 and 2017) conditions

		2011	2012	2016	2017
Parents	Min	50.00	55.00	65.00	61.00
	Max	55.00	60.00	74.00	71.00
	Mean	52.00	57.63	68.00	64.63
MAGIC population	Min	44.00	48.00	57.00	55.00
	Max	73.00	75.00	95.00	88.00
	Mean	53.73	59.91	68.00	69.00
	SE	0.16	0.17	0.22	0.20
	SD	3.85	3.96	5.02	4.69
	CV	14.82	15.64	25.19	21.98
	h^2		0.47		0.63

CV, Coefficient of variation; h^2 , heritability (for years 2011 and 2012; 2016 and 2017); Max, maximum; Min, minimum; SD, standard deviation (%); SE, standard error.

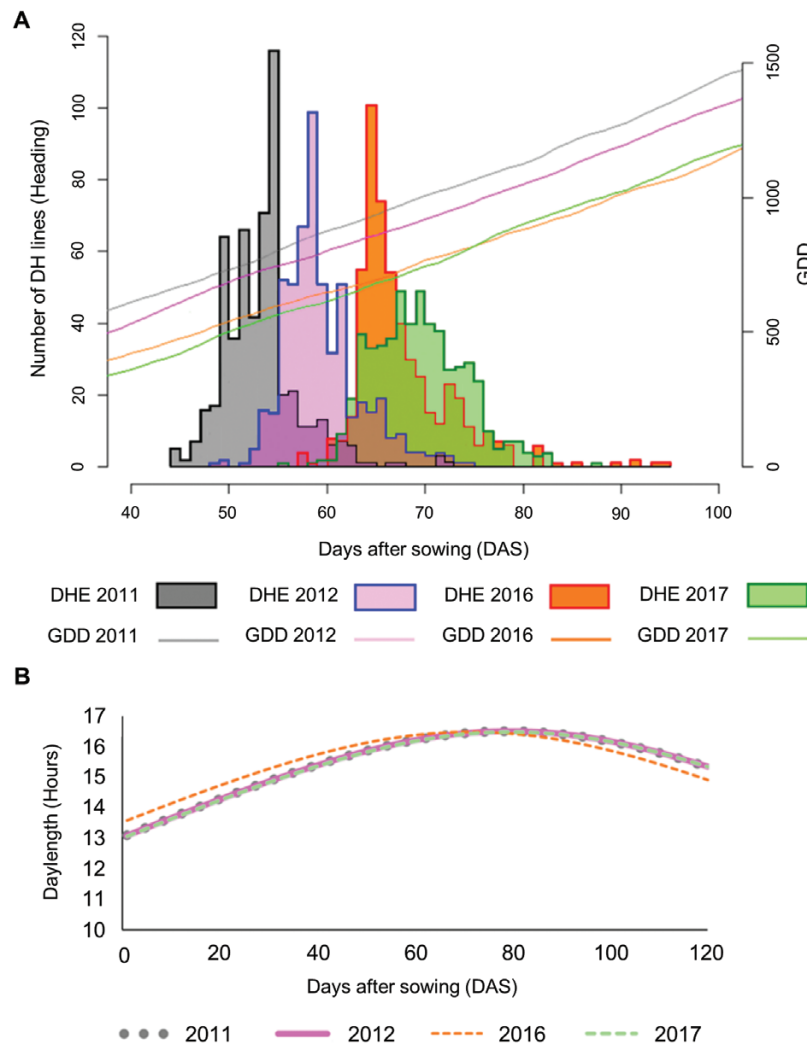


Fig. 1. (A) Comparison of flowering time (days to heading) distribution and GDD values for the years 2011, 2012, 2016 and 2017. (B) Comparison of day length in the same 4 years. (This figure is available in colour at JXB online.)

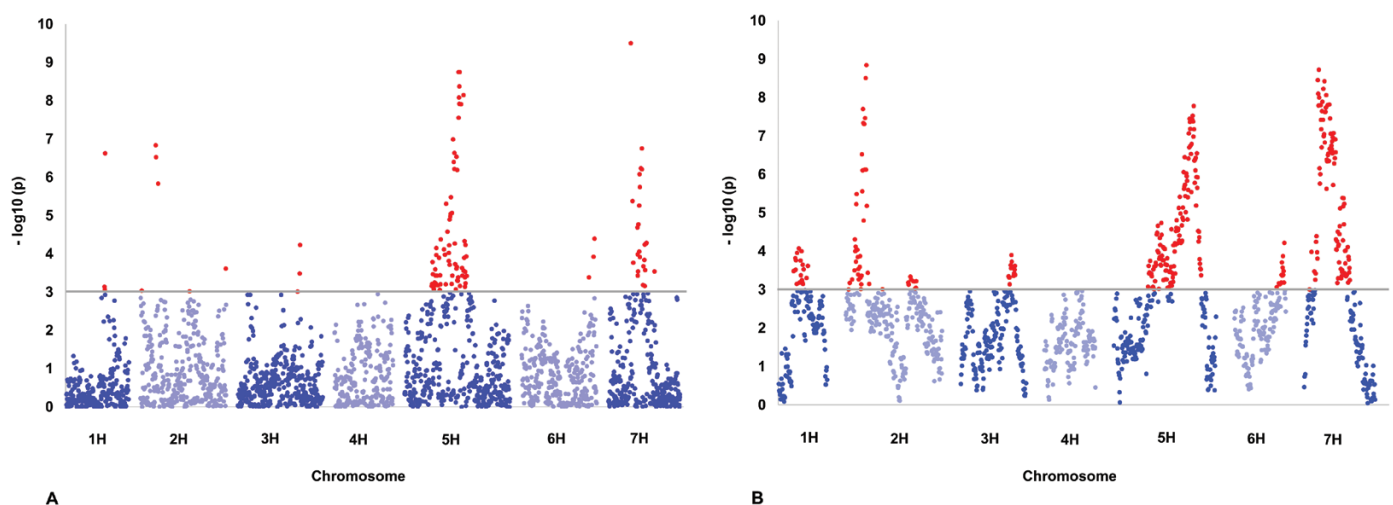


Fig. 2. Manhattan plots for (A) the single SNP approach and (B) haplotype approach for the spring barley MAGIC population grown under field conditions. The y axes denote the significance of SNP markers as $-\log_{10}(P)$ for flowering time (days to heading) in the barley population; the chromosomes are denoted on the x axes. The highlighted SNP markers above the cut-off line are significant by a threshold of $P \leq 0.001$ with 1000 permutations plus 20 times cross-validation. (This figure is available in colour at JXB online.)

Table 2. Significant QTLs associated with flowering time in the single SNP approach under field conditions

QTL	Peak marker ^a	Chr ^b	cM ^c	mbp ^d	Flanking re-gion (cM) ^e	F	P	FDR	Var (%) ^f	Parent ^g	MAF ^h	SNP1/ effect ⁱ	SNP2/ effect ^j	Gene ^k
HvHeading-1H-SA	BOPA1_1016_376	1H	71.03	480.40	70.89–71.030	35.76	2.33E-07	3.89E-05	6.37	2	0.08	G/3.82	A/-0.38	
HvHeading-2H-SA	SCRI_RS_233272	2H	18.91	27.30	18.91–23.80	41.19	1.43E-07	3.05E-05	7.22	8	0.02	T/-8.79	G/0.36	Ppd-H1
HvHeading-2H.2-SA	BOPA1_ABC14531_1_2_91	2H	91.21	687.20	91.21	15.56	9.31E-04	1.00E-02	2.88	1, 8	0.22	A/1.52	G/-0.38	denso/
HvHeading-3H-SA	SCRI_RS_103215	3H	109.21	634.07	108.85–109.21	24.73	5.8E-05	3.00E-03	4.48	3	0.1	A/-0.02	G/3.17	sdw1
HvHeading-5H-SA	SCRI_RS_152347	5H	69.31	522.50	69.31–74.93	18.91	1.62E-04	6.00E-03	3.4	8	0.14	A/2.06	G/-0.11	
HvHeading-5H.2-SA	SCRI_RS_204275	5H	80.21	543.30	77.52–85.56	22.06	6.96E-05	4.00E-03	3.91	1, 3, 8	0.49	C/-0.67	A/1.04	
HvHeading-5H.3-SA	BOPA2_12_21471	5H	122.43	595.20	118.89–128.54	53.97	1.78E-09	1.39E-06	9.22	8	0.17	G/2.73	A/-0.63	Vrn-H1
HvHeading-6H-SA	SCRI_RS_9648	6H	118.98	577.00	118.56–118.98	23.85	4.00E-05	3.00E-03	4.23	2, 5	0.31	A/-1.29	C/0.73	
HvHeading-7H-SA	BOPA2_12_30895	7H	34.35	39.70	34.35	60.33	3.14E-10	7.32E-07	9.96	8	0.04	C/5.79	G/-0.17	Vrn-H3
HvHeading-7H.2-SA	BOPA1_1107_392	7H	65.44	109.70	61.33–70.96	42.66	1.73E-07	3.36E-05	7.34	8	0.13	A/3.14	C/-0.35	HvCO1
HvHeading-7H.3-SA	BOPA1_ABC10040_1_1_238	7H	76.47	501.80	70.33–76.47	26.15	5.12E-05	3.00E-03	4.58	8	0.10	G/2.99	A/-0.26	
Total									48.43					

^a Most significant marker associated with the QTL.
^b The chromosome on which the QTL was located.
^c Genetic position of the most significant QTL according to Comadran et al. (2012).
^d Physical position of the most significant QTL according to barley pseudomolecules genome assembly (Beier et al., 2017; Mascher et al., 2017).
^e The range of the QTL interval according to Comadran et al. (2012).
^f Cross-validated proportion of the explained genetic variance of the QTL.
^g The parent(s) carrying the allele with lower frequency: 1, Ack. Bavaria; 2, Ack. Danubia; 3, Barke; 4, Crievenner; 5, Heils Franken; 6, Heines Hanna; 7, Pflugs Intensiv; 8, Ragusa.
^h Minor allele frequency
ⁱ Flowering effect of allele with lower frequency (days).
^j Flowering effect of allele with higher frequency (days).
^k Candidate gene corresponding to the QTL.

Table 3. Significant QTLs associated with flowering time in the haplotype approach under field conditions

QTL	Peak marker ^a	Chr ^b	cM ^c	Flanking region (cM) ^d	F	P	FDR	Var (%) ^e	Parent 1 ^f	Parent 2 ^f	Parent 3 ^f	Parent 4 ^f	Parent 5 ^f	Parent 6 ^f	Parent 7 ^f	Gene ^g
HvHeading-1H-HA	BOPA2_12_30147	1H	66.86	60.84–86.47	6.72	8.27E-05	6.72E-04	7.79	0.59	3.82	-0.44	-0.73	-0.38	-0.05	0.11	
HvHeading-2H-HA	SCRL_RS_140819	2H	27.69	3.82–53.75	13.61	1.42E-09	9.77E-07	14.96	-0.22	2.31	-0.39	-0.58	0.19	0.40	-8.79	Ppd-1
HvHeading-2H2-HA	SCRL_RS_160958	2H	92.78	91.15–99.26	5.25	4.54E-04	2.24E-03	6.25	0.66	-3.37	-1.04	-3.33	-0.17	-0.05	2.45	
HvHeading-3H-HA	BOPA1_ABC13753-1-2-167	3H	105.31	100.71–109.84	6.37	1.24E-04	9.14E-04	7.10	-1.00	-0.08	2.42	-0.29	0.45	-0.91	0.36	denso/sdw1
HvHeading-5H-HA	BOPA2_12_30377	5H	125.76	95.90–131.94	10.79	1.63E-08	1.43E-06	11.34	-1.15	-0.49	-0.37	-0.98	-0.05	0.05	3.00	Vrn-H1
HvHeading-6H-HA	SCRL_RS_144034	6H	119.33	116.15–119.33	6.07	5.96E-05	5.21E-04	7.67	1.48	-1.29	0.19	0.99	-1.14	-1.14	2.34	
HvHeading-7H-HA	BOPA1_	7H	37.61	23.80–67.42	12.63	1.87E-09	9.77E-07	12.65	-0.73	-1.07	-2.31	0.63	0.22	0.70	3.91	Vrn-H3
Total	ConsensusGBS0356-1							52.92								

^a Most significant marker associated with the QTL.
^b The chromosome that the QTL was located.
^c Genetic position of the most significant QTL according to Comadran et al. (2012)
^d The range of the QTL interval according to Comadran et al. (2012)
^e Cross-validated proportion of the explained genetic variance of the QTL.
^f Effect of allele for each parent (days) in reference to flowering time mean of the population: 1, Ack. Bavaria; 2, Ack. Danubia; 3, Barke; 4, Crievenner/Pflugs Intensiv; 5, Heils Franken; 6, Heines Hanna; 7, Ragusa.
^g Candidate gene corresponding to the QTL.

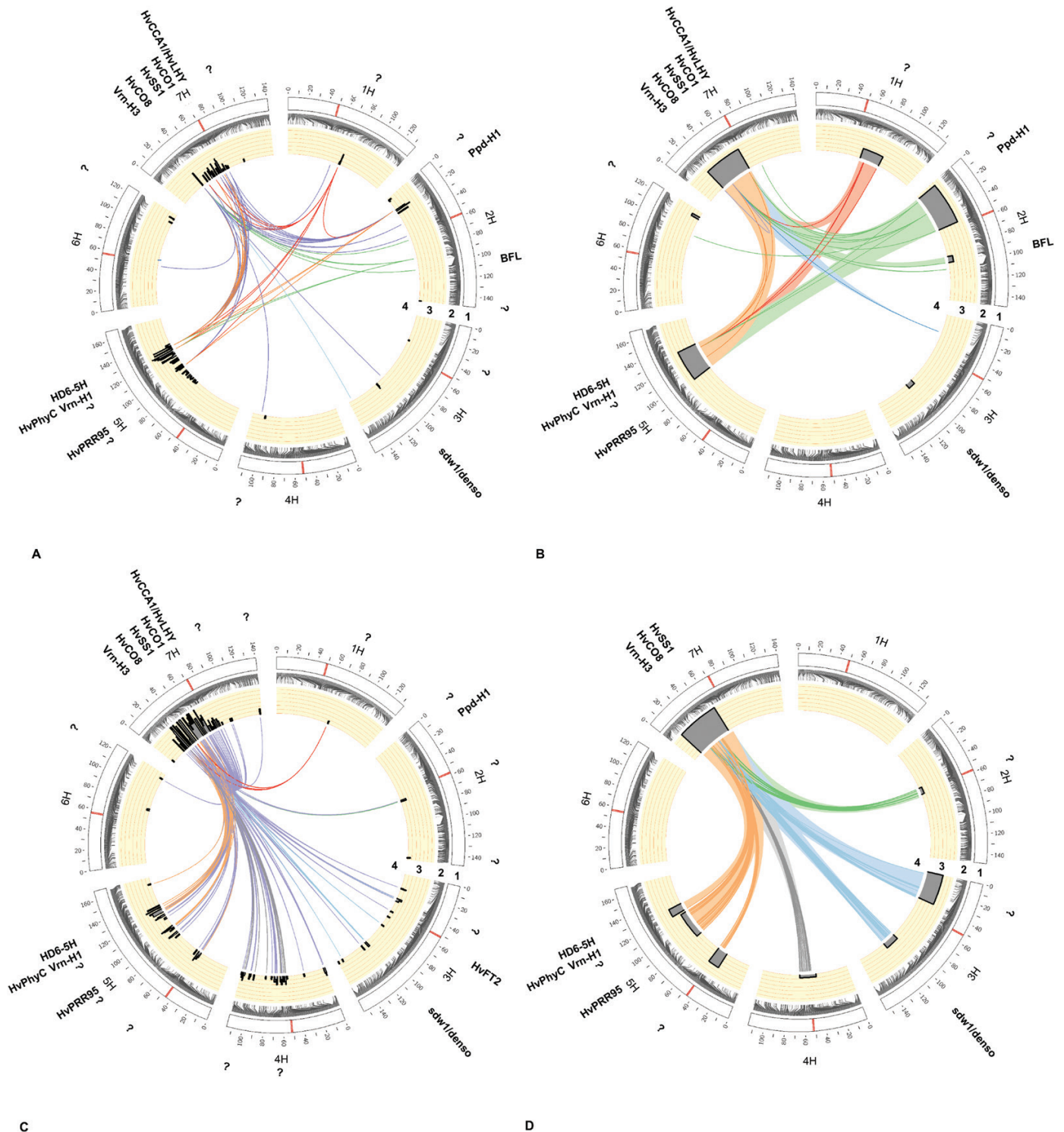


Fig. 3. Genetic composition of flowering time in a spring barley MAGIC population under field conditions, (A) single SNP approach and (B) haplotype approach, and under foil tunnel conditions, (C) single SNP approach and (D) haplotype approach. The candidate genes that might correspond to QTLs and digenic interactions are indicated outside the plots. 1, Barley chromosomes are shown as white bars and centromeres are highlighted within these bars. 2, Genetic position of SNPs on the chromosomes. 3, Probability of QTLs detected with $P \leq 0.001$ and 1000 permutations plus cross-validation via multilocus QTL analysis are shown as peak SNPs in SA and peak SNPs/interval (blocks) in HA. 4, Bridges in the center of each circle represent detected digenic interactions between SNP markers with $P \leq 0.1E-15$ via cross-validated multilocus epistatic interaction analysis. Question marks indicate loci where no genes for flowering time have been reported so far. Plots were drawn by Circos (Krzywinski et al., 2009). (This figure is available in colour at JXB online.)

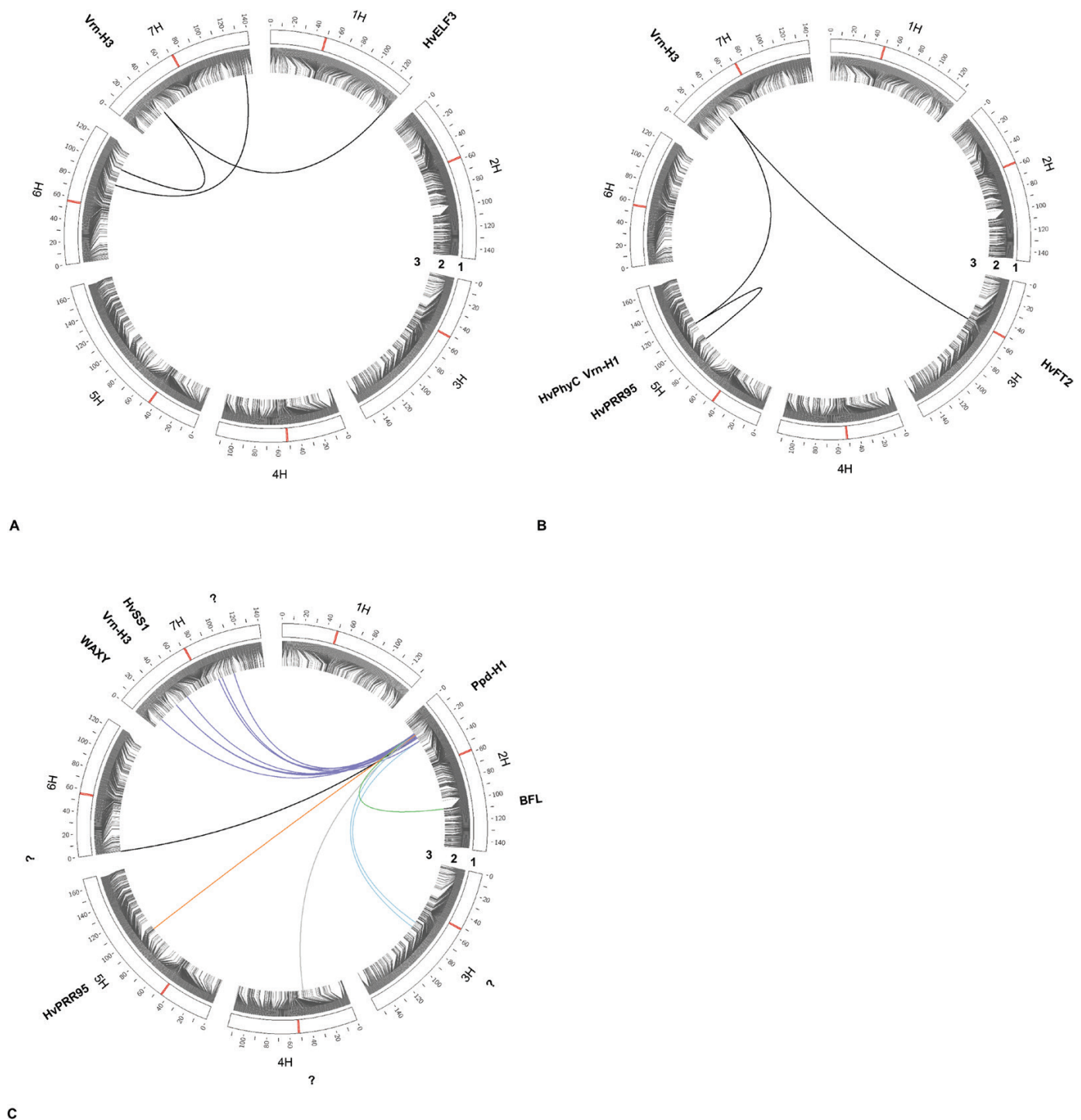


Fig. 4. Epistasis × environment interactions for flowering time in a spring barley MAGIC population by SA in (A) field conditions, (B) foil tunnel conditions, and (C) both field and foil tunnel conditions (4 years). Candidate genes that might correspond to QTLs and digenic interactions are indicated outside the plots. 1, Barley chromosomes are shown as white bars and centromeres are highlighted within these bars. 2, Genetic position of SNPs on the chromosomes. 3, Bridges in the center of each circle represent detected digenic interactions between SNP markers (A and B, $P \leq 0.1E-6$; C, $P \leq 0.1E-27$) via cross-validated multilocus epistatic interaction analysis. Question marks indicate loci where no genes for flowering time have been reported so far. Plots were drawn by Circos (Kryzwicki *et al.*, 2009). (This figure is available in colour at JXB online.)

allele with a flowering-delaying effect on chromosome 1H, which explained 6.37% (Table 2) and 7.79% (Table 3) of the genetic variation, respectively. We named this QTL HvHeading. The QTL allele segregated from the parent Danubia and was located within interval 70.89–71.03 cM

(BOPA1-1016–376, 71.03 cM) by SA (Table 2) and 60.84–86.47 cM (BOPA2_12_30147, 66.86 cM) by HA (Table 3). Analysis of allelic effect showed that as a single QTL it delayed flowering time by up to 3.82 days compared with the population average.

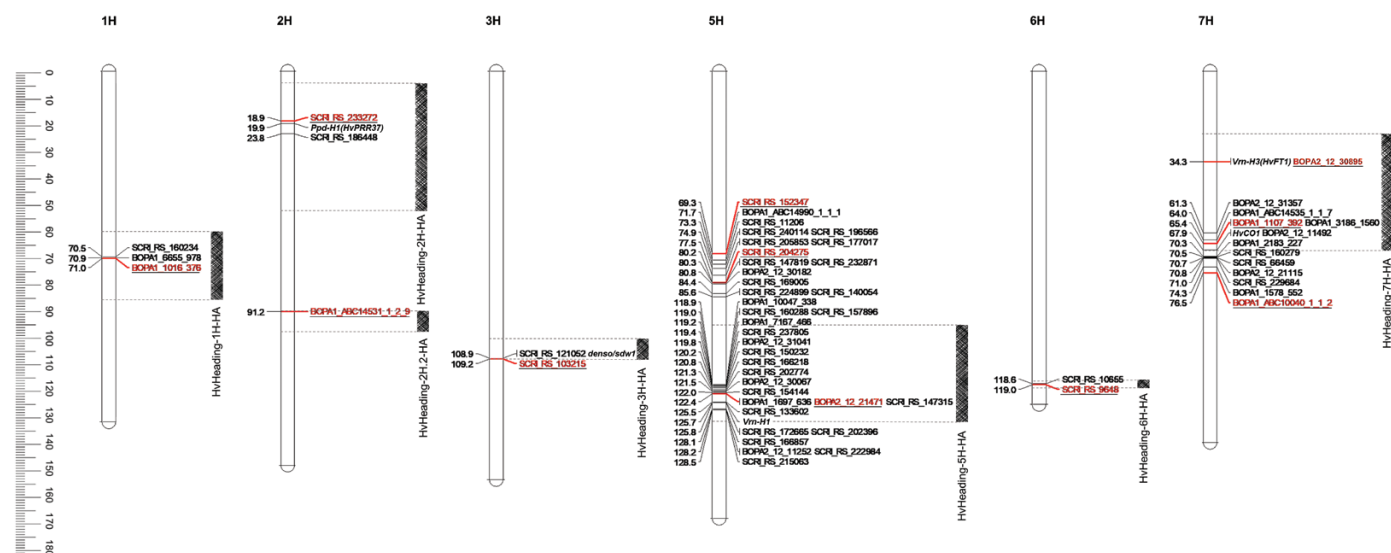


Fig. 5. Genetic map of QTLs for flowering time in spring barley MAGIC DH lines. Barley chromosomes are represented by white bars. The most significant SNP marker for each QTL according to SA is highlighted and underlined. The position of the haplotype that is associated with the QTL according to HA is shown with grey hatched blocks accompanied by the name of the corresponding QTL. Italicized gene names indicate the position of major flowering time genes as described for the Barke × Morex RILs by Mascher et al. (2013). The ruler on the left shows the chromosome length. (This figure is available in colour at JXB online.)

Several loci were involved in epistatic interactions with HvHeading (Fig. 3). SA revealed that in field conditions, an interaction of HvHeading with one locus on chromosome 7H, 34.35 cM (BOPA2_12_30895) could postpone flowering time by 12.38 days, while its interaction with a locus on chromosome 2H, 18.91 cM (SCRI_RS_233272) could accelerate flowering time by up to 10 days (Table 3 at Dryad). HA showed that interaction of the allele from Danubia with locus 7H, 37.61 cM (SCRI_RS_155061, interval 27.79–67.42 cM) from Ragusa could delay flowering time by 10.83 days, while its interaction with locus 2H, 27.69 cM (SCRI_RS_140819, interval 3.82–53.75 cM) from Ragusa could advance flowering by 10 days (Table 4 at Dryad). According to SA, under foil tunnel conditions HvHeading strongly interacted with several loci (Table 5 at Dryad). The most significant interaction was with the locus at 7H, 32.79 cM (BOPA1_12701_485), which could influence flowering time by 3.36 days.

To perform *in silico* analysis, the overlapping region between the QTL intervals from SA (7 cM) and HA (30 cM) was determined. The *in silico* approach revealed 160 annotated genes with predicted function in this region with different Gene Ontology annotations.

Influence of environment on flowering time

To evaluate the effect of environment on flowering time, the interaction of single and epistatic QTLs with the four environments was analyzed. The QTL × environment interaction analysis showed no significant effects under field conditions for both years. However, under foil tunnel conditions one QTL on chromosome 2H was detected by SA (19.90 cM) and HA (23.02 cM) (Tables 7 and 8 at Dryad). Considering all 4 years, SA and HA identified the most prominent region that interacted with environment on chromosome 2H (19.90

cM) and 7H (31.37 cM), respectively (Tables 9 and 10 at Dryad).

Analysis of epistasis × environment interactions using SA revealed 86 interactions with environment under field conditions (Table 11 at Dryad). Position 34.35 cM on chromosome 7H was involved in highly significant interactions (Fig. 4A). Analysis of epistasis × environment interactions in foil tunnel conditions by SA showed that 527 epistatic interactions were affected by environment, including HvHeading. The prominent regions involved in the 10 strongest interactions were located on chromosomes 5H (84.38–122.01 cM) and 7H (28.98–62.18 cM) (Fig. 4B; Table 12 at Dryad). No significant interactions were found when evaluating epistasis × environment interactions via HA. Across all 4 years, strong epistasis × environment interactions were detected (Table 13 at Dryad), which involved the interval located on chromosome 2H at 18.9–23.8 cM (Fig. 4C). Interactions of HvHeading with loci on chromosomes 2H, (SCRI_RS_233272, 18.9 cM), 7H (BOPA1_12701_485, 32.79 cM), and 5H (BOPA2_12_21471, 122.43 cM) were highly affected by environment (Table 14 at Dryad).

Discussion

Power of QTL and epistatic interaction analysis in a MAGIC population

Genetic mapping showed that the single SNP approach precisely pinpointed loci that represent prominent flowering time genes. The peak marker BOPA2-12-30895 on chromosome 7H is located in the *Vrn-H3* gene (Colmsee et al., 2015). This finding, as well as the detection by both SA and HA of QTLs and epistatic interactions that corresponded to previously described flowering time genes, is a proof of concept for the

power of the spring barley MAGIC population and the mixed linear model approach used in this study.

SA has been predominantly performed in QTL studies that used biparental populations or association panels (Xu *et al.*, 2017). However, in multiparental populations, if more than two parents are involved, SA is not able to unambiguously identify the parental origin of a given allele (i.e. SNP). This drawback can be overcome by using HA, which has offered a more informative evaluation of associated loci (Huang and George, 2011; Sannemann *et al.*, 2015; Ogawa *et al.*, 2018). In the present study, HA provided an estimation of allelic effect of each parent and, due to the potential contribution of all SNP information in one haplotype block, it produced smoother *P*-value plots (Fig. 2B) and created larger QTL intervals (Fig. 5) compared with SA. The presence of more markers in these QTL intervals allowed for the higher explanatory power of HA. This was in agreement with previous reports stating that marker–trait associations based on haplotype-phase data detected more SNPs associated with the trait (Sannemann *et al.*, 2015; N'Diaye *et al.*, 2017; Ogawa *et al.*, 2018).

Higher resolution of ‘haplotype-phasing’ data is mandatory for greater precision in mapping and depends on the linkage disequilibrium of the population, which is affected by the population size, diversity among the parents, population structure, marker density, and recombination frequency (Wang *et al.*, 2002). Considering the nature of the MAGIC population, including the presence of similarity among the founders, more cross-over rounds will not guarantee a greater number of assigned genetic regions (Stadlmeier *et al.*, 2018). One of the challenges during the current research was the construction of high-resolution haplotype data. Performing manual corrections clarified part of the unassigned regions, which shows that the existing algorithms for haplotype-phasing need to be improved to avoid wasting available data. Therefore, besides attempts to increase the number of cross-overs in the analyzed populations, developing an efficient haplotype-phase algorithm to maximize the usability of existing data seems to have a high priority in future studies.

The spring barley MAGIC DH lines supplied unique and diverse genetic material. The lower or higher than expected frequency (12.5%) for some SNP alleles might be due to the limited number of viable seeds obtained from the newly produced DH lines in the first round of cultivation.

Flowering time QTLs in the spring barley MAGIC population

Collectively, 18 QTLs were detected by SA and HA, including the QTL on chromosome 1H, which we named HvHeading, and nine QTLs that correspond to known flowering time genes. Due to the different data resolution of the two analyses, SA and HA found the same reported key genes for flowering time regulation at slightly varying genetic positions, suggesting that the novel region detected by both approaches on chromosome 1H has the same underlying gene. A region was mapped on chromosome 2H (18.91 cM, SA; 27.69 cM, HA) corresponding to the position of *Ppd-H1* (*HvPRR37*) (Alqudah *et al.*,

2014; Maurer *et al.*, 2015). The QTL detected on chromosome 3H (109.21 cM, SA; 105.31 cM, HA) was located in the region harboring the semi-dwarf gene *denso/sdw1* (Wang *et al.*, 2010; Maurer *et al.*, 2015, 2016; Sannemann *et al.*, 2015; Alqudah *et al.*, 2016). Furthermore, an interval on chromosome 5H (122.43 cM, SA; 125.76 cM, HA) was mapped to the position of the vernalization-response gene *Vrn-H1* (Wang *et al.*, 2010; Alqudah *et al.*, 2014; Maurer *et al.*, 2015; Sannemann *et al.*, 2015), and the detected region on chromosome 7H (34.35 cM, SA; 37.61 cM, HA) matched the position of another major vernalization-response gene, *Vrn-H3* (*HvFT1*) (Wang *et al.*, 2010; Alqudah *et al.*, 2014; Maurer *et al.*, 2015; Sannemann *et al.*, 2015).

Epistatic interactions in field and semi-controlled conditions

Different epistatic interactions were detected in field and semi-controlled conditions. The locus corresponding to *Vrn-H3* had the strongest epistatic interaction in both environments irrespective of the genetic approach used for analysis.

In field conditions, regions corresponding to *Vrn-H3* and *Ppd-H1* had the strongest epistatic interaction. It has been reported that *Ppd-H1* advances flowering time under long-day conditions by promoting *Vrn-H3* (Yan *et al.*, 2006). The epistatic interactions that involved the *Ppd-H1* region from Ragusa accelerated flowering time remarkably, showing an early-flowering haplotype-specific effect. The most significant epistatic interaction in foil tunnel conditions was among regions that corresponded to *Vrn-H3* and *Vrn-H1*. *Vrn-H1* seems to respond to low and high temperatures and is known to up-regulate *Vrn-H3* (Fu *et al.*, 2005; von Zitzewitz *et al.*, 2005; Gol *et al.*, 2017).

These results support previous descriptions of complex genetic networks in the flowering time pathway in barley (Maurer *et al.*, 2015). Epistatic interaction analysis for the different environments suggested that the flowering time of the MAGIC population was shaped by distinctive digenic interactions that adapt the DH lines to various environments.

HvHeading and participation in epistatic interactions

HvHeading, a novel flowering-delaying QTL allele, originated from the parental line Danubia. HvHeading was involved in significant epistatic interactions with loci that correspond to positions of major genes such as *Ppd-H1*, *Vrn-H1*, *Vrn-H3*, *sdw1/denso*, *HvPRR95*, *HvPhyC*, *HvCO8*, and *HvSS1*, indicating that it might have a major role in controlling flowering time in barley.

The closest known candidate gene to this QTL is *Ppd-H2* (*HvFT3*) at 93.1 cM (Halliwell *et al.*, 2016), which is involved in the photoperiod response under short-day conditions (Casao *et al.* 2011). Nevertheless, no association was detected between the region and flowering time in the spring barley MAGIC DH lines.

In silico analysis revealed several genes within the QTL interval that were annotated for families involved in flowering time, such as the MADS-box transcription factor protein (Trevaskis

et al., 2003), basic-leucine zipper (bZIP) transcription factor protein (Abe, 2005), FAR1 (Hudson et al., 1999), and OVATE (Wang et al., 2016) families. Further analysis is needed to identify and characterize the gene underlying HvHeading and its role in the flowering time pathway.

Epistasis × environment interactions and involvement of HvHeading

The different times of flowering in field and semi-controlled conditions were linked to environmental factors. The plants in the foil tunnel condition were exposed to higher temperatures compared with those in the field, resulting in a faster accumulation of GDD, which accelerated flowering time.

Analyzing QTL × environment interactions across the four environments (i.e. all 4 years) revealed a strong interaction of QTL regions harboring *Ppd-H1* and *Vrn-H3*. The results of epistasis × environment interaction analysis for the four environments also showed that most of the interactions had *Ppd-H1* region in common. *Ppd-H1* and *Vrn-H3* are both promoted by temperature (Turner et al., 2005; Yan et al., 2006), and recently it was reported that higher ambient temperature triggers *Ppd-H1* (Ejaz and von Korff, 2017). The detection of an interaction of *Vrn-H3* with the environment suggests that the outstanding effect of *Vrn-H3* in epistatic interactions under foil tunnel conditions could be due to the warmer environment. Epistasis × environment interactions showed that under foil tunnel conditions, loci corresponding to *Vrn-H1*, *HvPRR95*, and *Vrn-H3* were prominent, which supports previous reports that higher temperature triggers *Vrn-H1* and the downstream gene *Vrn-H3* (Karsai et al., 1997; Yan et al., 2003; von Zitzewitz et al., 2005; Ejaz and von Korff, 2017; Gol et al., 2017), which engage in a positive feedback loop that leads to early flowering under long-day conditions (Distelfeld et al., 2009).

HvHeading showed strong effects in epistasis × environment interactions in all four environments. It was involved in interactions with regions harboring *Ppd-H1*, *Vrn-H3*, and *Vrn-H1*, suggesting that HvHeading might have an effect on flowering time via an interaction with temperature.

Conclusion

Flowering time in barley is ultimately controlled by interactions among genes that can take different routes depending on environmental cues to adapt and fulfill timely flowering. The spring barley MAGIC population provided a genetic depth and richness that was required to study the effect of epistasis and environment interactions on complex traits such as flowering time. The results highlighted flowering time modulators as well as one novel QTL allele, HvHeading, that strongly interacted with regions corresponding to the *Vrn-H3*, *Vrn-H1*, and *Ppd-H1* genes that are at the intersection of other genetic competitors. Further studies are needed to elaborate the underlying gene (or genes) and decipher its role and function in the pathway by shedding light on its interaction with other genetic and environmental factors.

Data availability

The following data are available at Dryad Digital Repository: <https://doi.org/10.5061/dryad.g25cm28>.

Dataset 1. Phenotypic data for days to heading (4 years) using MAGIC DH lines.

Dataset 2. Growing degree-days (GDD) during 100 days after sowing (2011, 2012, 2016, and 2017).

Dataset 3. Genotyping data by barley 9k iSelect SNP array using MAGIC DH lines.

Methods 1. SAS script and sample data for haplotype construction by the K-means clustering method.

Methods 2. SAS script for QTL and epistasis mapping process as well as environment interaction analysis including implementation of FDR and cross-validation procedures.

Table 1. Analysis of variance for 534 MAGIC DH lines.

Table 2. Descriptive statistics for growing degree-days (GDD) during 100 days after sowing.

Table 3. Epistatic interactions by single SNP approach under field conditions.

Table 4. Epistatic interactions by haplotype approach under field conditions.

Table 5. Epistatic interactions by single SNP approach under foil tunnel conditions.

Table 6. Epistatic interactions by haplotype approach under foil tunnel conditions.

Table 7. QTL × environment interactions by single SNP approach under foil tunnel conditions.

Table 8. QTL × environment interactions by haplotype approach under foil tunnel conditions.

Table 9. QTL × environment interactions by single SNP approach for 4 years (field and foil tunnel conditions).

Table 10. QTL × environment interactions by haplotype approach for 4 years (field and foil tunnel conditions).

Table 11. Epistasis × environment interactions by single SNP approach under field conditions.

Table 12. Epistasis × environment interactions by single SNP approach under foil tunnel conditions.

Table 13. Epistasis × environment interactions by single SNP approach for 4 years.

Table 14. Epistasis × environment interactions that engaged peak marker for HvHeading (BOPA1_1016_376) by single SNP approach for 4 years.

Acknowledgements

We thank the German Research Foundation (DFG) for funding this research under priority program 1530, 'Flowering time control: from natural variation to crop improvement'.

References

- Abe M, Kobayashi Y, Yamamoto S, Daimon Y, Yamaguchi A, Ikeda Y, Ichinoki H, Notaguchi M, Goto K, Araki T. 2005. FD, a bZIP protein mediating signals from the floral pathway integrator FT at the shoot apex. *Science* **309**, 1052–1056.
- Afsharyan NP, Sannemann W, Léon J, Ballvora A. 2020. Data from: Effect of epistasis and environment on flowering time in barley reveals a

novel flowering-delaying QTL allele. Dryad Digital Repository. doi: 10.5061/dryad.g25cm28.

Alqudah AM, Koppolu R, Wolde GM, Graner A, Schnurbusch T. 2016. The genetic architecture of barley plant stature. *Frontiers in Genetics* **7**, 117.

Alqudah AM, Sharma R, Pasam RK, Graner A, Kilian B, Schnurbusch T. 2014. Genetic dissection of photoperiod response based on GWAS of pre-anthesis phase duration in spring barley. *PLoS One* **9**, e113120.

Bandillo N, Raghavan C, Muycio PA, et al. 2013. Multi-parent advanced generation inter-cross (MAGIC) populations in rice: progress and potential for genetics research and breeding. *Rice* **6**, 11.

Bauer AM, Hoti F, von Korff M, Pillen K, Léon J, Sillanpää MJ. 2009. Advanced backcross-QTL analysis in spring barley (*H. vulgare* ssp. *spontaneum*) comparing a REML versus a Bayesian model in multi-environmental field trials. *Theoretical and Applied Genetics* **119**, 105–123.

Beier S, Himmelbach A, Colmsee C, et al. 2017. Construction of a map-based reference genome sequence for barley, *Hordeum vulgare* L. *Scientific Data* **4**, 170044.

Bezant J, Laurie D, Pratchett N, Chojecki J, Kearsey M. 1996. Marker regression mapping of QTL controlling flowering time and plant height in a spring barley (*Hordeum vulgare* L.) cross. *Heredity* **77**, 64–73.

Blümel M, Dally N, Jung C. 2015. Flowering time regulation in crops—what did we learn from Arabidopsis? *Current Opinion in Biotechnology* **32**, 121–129.

Browning SR, Browning BL. 2011. Haplotype phasing: existing methods and new developments. *Nature Reviews. Genetics* **12**, 703–714.

Campoli C, Drosse B, Searle I, Coupland G, von Korff M. 2012. Functional characterisation of *HvCO1*, the barley (*Hordeum vulgare*) flowering time ortholog of *CONSTANS*. *The Plant Journal* **69**, 868–880.

Casao MC, Karsai I, Igartua E, Gracia MP, Veisz O, Casas AM. 2011. Adaptation of barley to mild winters: a role for *PPDH2*. *BMC Plant Biology* **11**, 164.

Cockram J, Horsnell R, Soh E, Norris C, O'Sullivan DM. 2015. Molecular and phenotypic characterization of the alternative seasonal growth habit and flowering time in barley (*Hordeum vulgare* ssp. *vulgare* L.). *Molecular Breeding* **35**, 165.

Cockram J, Jones H, Leigh FJ, O'Sullivan D, Powell W, Laurie DA, Greenland AJ. 2007. Control of flowering time in temperate cereals: genes, domestication, and sustainable productivity. *Journal of Experimental Botany* **58**, 1231–1244.

Cavanagh C, Morell M, Mackay I, Powell W. 2008. From mutations to MAGIC: resources for gene discovery, validation and delivery in crop plants. *Current Opinion in Plant Biology* **11**, 215–221.

Colmsee C, Beier S, Himmelbach A, Schmutzer T, Stein N, Scholz U, Mascher M. 2015. BARLEX – the barley draft genome explorer. *Molecular Plant* **8**, 964–966.

Comadran J, Kilian B, Russell J, et al. 2012. Natural variation in a homolog of *Antirrhinum CENTRORADIALIS* contributed to spring growth habit and environmental adaptation in cultivated barley. *Nature Genetics* **44**, 1388–1392.

Digel B, Pankin A, von Korff M. 2015. Global transcriptome profiling of developing leaf and shoot apices reveals distinct genetic and environmental control of floral transition and inflorescence development in barley. *The Plant Cell* **27**, 2318–2334.

Distelfeld A, Li C, Dubcovsky J. 2009. Regulation of flowering in temperate cereals. *Current Opinion in Plant Biology* **12**, 178–184.

Doerge RW, Churchill GA. 1996. Permutation tests for multiple loci affecting a quantitative character. *Genetics* **142**, 285–294.

Ejaz M, von Korff M. 2017. The genetic control of reproductive development under high ambient temperature. *Plant Physiology* **173**, 294–306.

Faure S, Higgins J, Turner A, Laurie DA. 2007. The *FLOWERING LOCUS T*-like gene family in barley (*Hordeum vulgare*). *Genetics* **176**, 599–609.

Federer WT. 1956a. A method for evaluating genetic progress in a sugar cane breeding program. *Hawaiian Planters' Record* **55**, 177–190.

Federer WT. 1956b. Augmented (or hoonuiaku) designs. *Hawaiian Planters' Record* **55**, 191–208.

Federer WT. 1993. Statistical design and analysis for intercropping experiments. New York: Springer-Verlag.

Fu D, Szucs P, Yan L, Helguera M, Skinner JS, von Zitzewitz J, Hayes PM, Dubcovsky J. 2005. Large deletions within the first intron

in *VRN-1* are associated with spring growth habit in barley and wheat. *Molecular Genetics and Genomics* **273**, 54–65.

Gol L, Tomé F, von Korff M. 2017. Floral transitions in wheat and barley: interactions between photoperiod, abiotic stresses, and nutrient status. *Journal of Experimental Botany* **68**, 1399–1410.

Hack H, Bleiholder L, Buhr L, Meier U, Schnock-Fricke U, Weber E, Witzemberger A. 1992. Einheitliche Codierung der phänologischen Entwicklungsstadien mono- und dikotyledoner Pflanzen. *Erweiterte BBCH-Skala*, Allgemeine. *Nachrichtenblatt des Deutschen Pflanzenschutzdienstes* **44**, 265–270.

Halliwel J, Borrill P, Gordon A, Kowalczyk R, Pagano ML, Saccomanno B, Bentley AR, Uauy C, Cockram J. 2016. Systematic investigation of *FLOWERING LOCUS T*-like Poaceae gene families identifies the short-day expressed flowering pathway gene, *TaFT3* in wheat (*Triticum aestivum* L.). *Frontiers in Plant Science* **7**, 857.

Hemming MN, Peacock WJ, Dennis ES, Trevaskis B. 2008. Low-temperature and daylength cues are integrated to regulate *FLOWERING LOCUS T* in barley. *Plant Physiology* **147**, 355–366.

Huang BE, George AW. 2011. R/mpMap: a computational platform for the genetic analysis of multiparent recombinant inbred lines. *Bioinformatics* **27**, 727–729.

Huang BE, George AW, Forrest KL, Kilian A, Hayden MJ, Morell MK, Cavanagh CR. 2012. A multiparent advanced generation inter-cross population for genetic analysis in wheat. *Plant Biotechnology Journal* **10**, 826–839.

Hudson M, Ringli C, Boylan MT, Quail PH. 1999. The *FAR1* locus encodes a novel nuclear protein specific to phytochrome A signaling. *Genes & Development* **13**, 2017–2027.

International Barley Genome Sequencing Consortium. 2012. A physical, genetic and functional sequence assembly of the barley genome. *Nature* **491**, 711–716.

Karsai I, Mészáros K, Hayes PM, Bedo Z. 1997. Effects of loci on chromosomes 2 (2H) and 7 (5H) on developmental patterns in barley (*Hordeum vulgare* L.) under different photoperiod regimes. *Theoretical and Applied Genetics* **94**, 612–618.

Kilpikari R, Sillanpää MJ. 2003. Bayesian analysis of multilocus association in quantitative and qualitative traits. *Genetic Epidemiology* **25**, 122–135.

King EG, Merkes CM, McNeil CL, Hooper SR, Sen S, Broman KW, Long AD, Macdonald SJ. 2012. Genetic dissection of a model complex trait using the *Drosophila* Synthetic Population Resource. *Genome Research* **22**, 1558–1566.

Kover PX, Valdar W, Trakalo J, Scarcelli N, Ehrenreich IM, Purugganan MD, Durrant C, Mott R. 2009. A multiparent advanced generation inter-cross to fine-map quantitative traits in *Arabidopsis thaliana*. *PLoS Genetics* **5**, e1000551.

Krzywinski M, Schein J, Birol I, Connors J, Gascoyne R, Horsman D, Jones SJ, Marra MA. 2009. Circos: an information aesthetic for comparative genomics. *Genome Research* **19**, 1639–1645.

Mackay IJ, Bansept-Basler P, Barber T, et al. 2014. An eight-parent multiparent advanced generation inter-cross population for winter-sown wheat: creation, properties, and validation. *G3* **4**, 1603–1610.

Mangelsdorf AJ. 1953. Sugarcane breeding in Hawaii. Part II. 1921 to 1952. *Hawaiian Planters' Record* **54**, 101–137.

Mascher M, Gundlach H, Himmelbach A, et al. 2017. A chromosome conformation capture ordered sequence of the barley genome. *Nature* **544**, 427–433.

Mascher M, Muehlbauer GJ, Rokhsar DS, et al. 2013. Anchoring and ordering NGS contig assemblies by population sequencing (POPSEQ). *The Plant Journal* **76**, 718–727.

Mathew B, Léon J, Sannemann W, Sillanpää MJ. 2018. Detection of epistasis for flowering time using Bayesian multilocus estimation in a barley MAGIC population. *Genetics* **208**, 525–536.

Maurer A, Draba V, Jiang Y, Schnaitmann F, Sharma R, Schumann E, Kilian B, Reif JC, Pillen K. 2015. Modelling the genetic architecture of flowering time control in barley through nested association mapping. *BMC Genomics* **16**, 290.

Maurer A, Draba V, Pillen K. 2016. Genomic dissection of plant development and its impact on thousand grain weight in barley through nested association mapping. *Journal of Experimental Botany* **67**, 2507–2518.

- Mouradov A, Cremer F, Coupland G.** 2002. Control of flowering time: interacting pathways as a basis for diversity. *The Plant Cell* **14**(Suppl), S111–S130.
- N'Diaye A, Haile JK, Cory AT, Clarke FR, Clarke JM, Knox RE, Pozniak CJ.** 2017. Single marker and haplotype-based association analysis of semolina and pasta colour in elite durum wheat breeding lines using a high-density consensus map. *PLoS One* **12**, e0170941.
- Ogawa D, Yamamoto E, Ohtani T, Kanno N, Tsunematsu H, Nonoue Y, Yano M, Yamamoto T, Yonemaru JI.** 2018. Haplotype-based allele mining in the Japan-MAGIC rice population. *Scientific Reports* **8**, 4379.
- Phillips PC.** 2008. Epistasis – the essential role of gene interactions in the structure and evolution of genetic systems. *Nature Reviews. Genetics* **9**, 855–867.
- Pillen K, Zacharias A, Léon J.** 2003. Advanced backcross QTL analysis in barley (*Hordeum vulgare* L.). *Theoretical and Applied Genetics* **107**, 340–352.
- Putterill J, Laurie R, Macknight R.** 2004. It's time to flower: the genetic control of flowering time. *BioEssays* **26**, 363–373.
- R Core Team.** 2015. R: a language and environment for statistical computing. Vienna: R Foundation for Statistical Computing.
- Ross-Ibarra J, Morrell PL, Gaut BS.** 2007. Plant domestication, a unique opportunity to identify the genetic basis of adaptation. *Proceedings of the National Academy of Sciences, USA* **104**(Suppl 1), 8641–8648.
- Rutkoski JE, Poland J, Jannink JL, Sorrells ME.** 2013. Imputation of unordered markers and the impact on genomic selection accuracy. *G3* **3**, 427–439.
- Sannemann W, Huang BE, Mathew B, Léon J.** 2015. Multi-parent advanced generation inter-cross in barley: high-resolution quantitative trait locus mapping for flowering time as a proof of concept. *Molecular Breeding* **35**, 86.
- Schelling K, Born K, Weissteiner C, Kühbauch W.** 2003. Relationships between yield and quality parameters of malting barley (*Hordeum vulgare* L.) and phenological and meteorological data. *Journal of Agronomy and Crop Science* **189**, 113–122.
- Schulte D, Close TJ, Graner A, et al.** 2009. The International Barley Sequencing Consortium—at the threshold of efficient access to the barley genome. *Plant Physiology* **149**, 142–147.
- Sillanpää MJ, Corander J.** 2002. Model choice in gene mapping: what and why. *Trends in Genetics* **18**, 301–307.
- Stadlmeier M, Hartl L, Mohler V.** 2018. Usefulness of a multiparent advanced generation intercross population with a greatly reduced mating design for genetic studies in winter wheat. *Frontiers in Plant Science* **871**, 1–12.
- Trevaskis B, Bagnall DJ, Ellis MH, Peacock WJ, Dennis ES.** 2003. MADS box genes control vernalization-induced flowering in cereals. *Proceedings of the National Academy of Sciences, USA* **100**, 13099–13104.
- Trione EJ, Metzger RJ.** 1970. Wheat and barley vernalization in a precise temperature gradient. *Crop Science* **10**, 390–392.
- Turner A, Beales J, Faure S, Dunford RP, Laurie DA.** 2005. The pseudo-response regulator Ppd-H1 provides adaptation to photoperiod in barley. *Science* **310**, 1031–1034.
- Valentim FL, Van Mourik S, Posé D, et al.** 2015. A quantitative and dynamic model of the Arabidopsis flowering time gene regulatory network. *PLoS One* **10**, 1–18.
- von Korff M, Wang H, Léon J, Pillen K.** 2006. AB-QTL analysis in spring barley: II. Detection of favourable exotic alleles for agronomic traits introgressed from wild barley (*H. vulgare* ssp. *spontaneum*). *Theoretical and Applied Genetics* **112**, 1221–1231.
- von Zitzewitz J, Szucs P, Dubcovsky J, Yan L, Francia E, Pecchioni N, Casas A, Chen TH, Hayes PM, Skinner JS.** 2005. Molecular and structural characterization of barley vernalization genes. *Plant Molecular Biology* **59**, 449–467.
- Wang N, Akey JM, Zhang K, Chakraborty R, Jin L.** 2002. Distribution of recombination crossovers and the origin of haplotype blocks: the interplay of population history, recombination, and mutation. *American Journal of Human Genetics* **71**, 1227–1234.
- Wang S, Chang Y, Ellis B.** 2016. Overview of OVATE FAMILY PROTEINS, a novel class of plant-specific growth regulators. *Frontiers in Plant Science* **7**, 1–8.
- Wang G, Schmalenbach I, von Korff M, Léon J, Kilian B, Rode J, Pillen K.** 2010. Association of barley photoperiod and vernalization genes with QTLs for flowering time and agronomic traits in a BC2DH population and a set of wild barley introgression lines. *Theoretical and Applied Genetics* **120**, 1559–1574.
- Warner JN.** 1953. The evolution of a philosophy on sugar cane breeding in Hawaii. *Hawaiian Planters' Record* **54**, 139–162.
- Xu Y, Li P, Yang Z, Xu C.** 2017. Genetic mapping of quantitative trait loci in crops. *The Crop Journal* **5**, 175–184.
- Yan L, Fu D, Li C, Blechl A, Tranquilli G, Bonafede M, Sanchez A, Valarik M, Yasuda S, Dubcovsky J.** 2006. The wheat and barley vernalization gene *VRN3* is an orthologue of *FT*. *Proceedings of the National Academy of Sciences, USA* **103**, 19581–19586.
- Yan L, Loukoianov A, Tranquilli G, Helguera M, Fahima T, Dubcovsky J.** 2003. Positional cloning of the wheat vernalization gene *VRN1*. *Proceedings of the National Academy of Sciences, USA* **100**, 6263–6268.